

# Robust Synthesis of Gold Nanotriangles and their Self-Assembly into Vertical Arrays

Piotr Szustakiewicz,<sup>[a, b]</sup> Guillermo González-Rubio,<sup>[b]</sup> Leonardo Scarabelli,<sup>[b, c]</sup> and Wiktor Lewandowski<sup>\*[a, b]</sup>

We report an efficient, seed-mediated method for the synthesis of gold nanotriangles (NTs) which can be used for controlled self-assembly. The main advantage of the proposed synthetic protocol is that it relies on using stable (over the course of several days) intermediate seeds. This stability translates into increasing time efficiency of the synthesis and makes the protocol experimentally less demanding ('fast addition' not required, tap water can be used in the final steps) as compared to previously reported procedures, without compromising the

size and shape monodispersity of the product. We demonstrate high reproducibility of the protocol in the hands of different researchers and in different laboratories. Additionally, this modified seed-mediated method can be used to produce NTs with edge lengths between ca. 45 and 150 nm. Finally, the high 'quality' of NTs allows the preparation of long-range ordered assemblies with vertically oriented building blocks, which makes them promising candidates for future optoelectronic technologies.

## 1. Introduction

Beveled triangular Au nanoprisms (truncated right bipyramids having a single twin defect called nanotriangles, NTs) have drawn a lot of attention due to their superior performance in the areas of biosensing,<sup>[1]</sup> self-assembly,<sup>[2]</sup> plasmon-exciton<sup>[3]</sup> and plasmon-trion<sup>[4]</sup> hybrid materials, opto-thermoplasmonic fluidics,<sup>[5]</sup> radiotherapy,<sup>[6]</sup> chemical sensing<sup>[7]</sup> and regioselective immobilization of biomolecules.<sup>[8]</sup> The main reason for such widespread applications of triangular gold nanoparticles (Au NPs) are their unique shape-dependent optoelectronic and self-assembly properties. For example highly curved corners ensure large electric field enhancements which are beneficial for sensing applications, while the triangular geometry imposes anisotropic optical properties.<sup>[7]</sup> Simultaneously, the triangular shape translates into a rich polymorphism of their self-assembled structures.<sup>[9]</sup> The growing interest in the use of triangular Au NPs requires detailed investigation and

development<sup>[10]</sup> of reliable and tunable methods for their synthesis,<sup>[11]</sup> purification<sup>[12]</sup> and self-assembly.<sup>[13]</sup>

It is worth to make a clear distinction between two types of Au nanoparticles with the overall triangular geometry: (i) triangular nanoplates (triangular-shaped nanoparticles that have two or more planar defects in a parallel arrangement called stacking faults)<sup>[14–16]</sup> and (ii) triangular nanoprisms / nanotriangles.<sup>[17,17]</sup> Due to the different internal structure the former are typically thin (<20 nm width) and large (100–300 nm length, although they can reach up to 1000 nm),<sup>[18]</sup> while nanotriangles are typically thicker (>20 nm) and smaller (50–180 nm edge length).<sup>[17]</sup> Localized surface plasmon resonances (LSPRs) of NTs range from 600 to 800 nm<sup>[17,19]</sup> while in the case of triangular nanoplates LSPR bands are located between 800 and 1300 nm.<sup>[14–16]</sup>

The synthesis of anisotropic nanoparticles in general is not an easy task due to the requirement of controlled symmetry breaking.<sup>[20]</sup> In the case of Au triangular nanoplates, several successful strategies have been developed.<sup>[14–16,21–23]</sup> In contrast, synthetic protocols for NTs are more seldom. One example is a high yield and quick, seedless, oxidative etching method.<sup>[24]</sup> Using this method, authors prepared a wide range of NTs of edge length between 40 to 120 nm and LSPR maxima at 620 to 700 nm. Importantly, these NTs exhibit low size dispersity, which supports their self-assembly.<sup>[9]</sup>

However, the development of seed-mediated approaches for NTs also appears appealing.<sup>[25,26,27]</sup> In principle, seed-mediated methods should enable precise and wide tuning of NTs size, continuous shift of the main LSPR band position, ensure shape control, and should be easily reproducible and scalable.

Seed-mediated approaches have already proven feasible to achieve NTs with controlled size and plasmonic properties. One possibility involves seed-less preparation of small NTs followed by seed-mediated growth in a second step. Along this line, Kuttner et al.<sup>[19]</sup> prepared NTs of edge length between 100 to

[a] P. Szustakiewicz, Dr. W. Lewandowski  
Faculty of Chemistry  
University of Warsaw  
Pasteura 1 st., Warsaw, 02-093, Poland  
E-mail: wlewandowski@chem.uw.edu.pl

[b] P. Szustakiewicz, Dr. G. González-Rubio, Dr. L. Scarabelli,  
Dr. W. Lewandowski  
CICbiomaGUNE  
Paseo de Miramón 182, Donostia-San Sebastián, 20014, Spain

[c] Dr. L. Scarabelli  
California NanoSystems Institute  
University of California, Los Angeles  
Los Angeles 90095 California, USA

Supporting information for this article is available on the WWW under <https://doi.org/10.1002/open.201900082>

©201x The Authors. Published by Wiley-VCH Verlag GmbH & Co. KGaA.  
This is an open access article under the terms of the Creative Commons Attribution Non-Commercial License, which permits use, distribution and reproduction in any medium, provided the original work is properly cited and is not used for commercial purposes.

180 nm and LSPR maxima at 590 to 740 nm. Uniquely, these NTs, exhibit constant aspect ratio for all sizes and narrow size distribution, while sharp tips allow their use in SERS sensing.

If NTs with sizes below 100 nm are required<sup>[28]</sup> the seed-mediated method described by Scarabelli et al.<sup>[17]</sup> seems most appealing. In this protocol, varied amounts of Au seeds stabilized with cetyltrimethylammonium chloride (CTAC) were used to prepare NTs with side-length ranging from 59 to 147 nm and LSPR maxima in the range 640 to 750 nm. This method is especially appealing, since it enables the synthesis of NTs with well-defined geometry, ensures high shape yields and enables upscaling, however it still suffers from the traditional problems of seed-mediated syntheses. A problem that is often encountered by those reproducing the protocol by Scarabelli et al.<sup>[17]</sup> (as well as other seed-mediated syntheses of nanoparticles) is the low stability of the seed particles. In other words, if you are to produce several batches of NTs (e.g. of different sizes), you should do it shortly after the synthesis of the initial seeds. Otherwise, you will have to start the protocol all over again, which is time consuming and can lower the reproducibility of your results. Another drawback is that the crucial step of this method relies on a fast addition technique, which can also affect reproducibility and shape yields in the hands of an inexperienced researcher and is highly dependent on the quality of water used.

Beyond synthesis, assembling anisotropic NPs into long-range ordered arrays with vertically oriented building blocks has attracted much attention as a frequently necessary step, on the way to practical applications.<sup>[7]</sup> Vertical assemblies of anisotropic NPs are promising since they expose highly curved surfaces, which is of great interest for hot-electron mediated catalysis and plasmonic sensing applications.<sup>[29]</sup> Methodologies for producing vertical assemblies are well developed for nanorods,<sup>[30–34]</sup> in the case of Au NTs, efficient production of such assemblies has been seldom obtained.<sup>[9,19]</sup>

Here, we introduce an improved variation of Scarabelli's protocol that resolves these issues by providing access to highly stable seeds that can be stored and used for a long period of time, without affecting the quality of the final product and offering various advantages. On one hand, with this improved protocol we were able to push the lower size limit of NTs in comparison to the current state-of-the-art seed-based methods. On the other hand, we demonstrate the user-friendly character of the protocol by reproducing it in a different laboratory, we describe an often overlooked impact of water quality on the final product,<sup>[35,36]</sup> confirm scale-up feasibility and introduce a two-step purification process for efficient purification of NTs larger than 100 nm. Finally, we show that the quality of the product allows us to prepare well-ordered, large area, mono- and bi-layer arrays of orientationally ordered NTs – vertical assemblies are prepared for NTs coated with hydrophilic ligands.

## 2. Results and Discussion

### 2.1. Seed Formation

In a previously devised protocol for NTs synthesis, some of us proposed a four stage seed mediated synthetic scheme.<sup>[17]</sup> In short, the protocol starts with the synthesis of small, spherical seeds, which are then aged for 2 hours (ageing is fundamental for increasing shape-yield of the synthesis<sup>[11]</sup>). Afterwards, the initial seeds are isotropically overgrown in the presence of iodide,<sup>[11,17]</sup> (formation of 'intermediate' seeds) and while still growing, these particles are quickly transferred (so-called 'fast addition') to the final growth solution, which ensures anisotropic growth. NTs of different sizes are obtained depending on the amount of the used seeds. In the final step, shape- and size-selective purification based on depletion forces allowed to achieve solutions of uniform nanotriangles.<sup>[11]</sup> Although successful in the terms of the quality of the product, this protocol suffers from two drawbacks: (I) the requirement to synthesize NTs shortly after obtaining the initial seeds, (II) the requirement to use a fast addition technique; both issues may translate into a low reproducibility of the protocol in the hands of an inexperienced researcher, especially if a set of NTs with different sizes will be produced over the course of few days (which is often the case). In such a case, the initial seeds need to be synthesized several times, which adds variability to the product, since the outcome of this synthesis step (and in turn the quality of the final product) is strongly dependent on factors such as the time lapse between NaBH<sub>4</sub> solution preparation and addition to the reaction mixture or how quickly the NaBH<sub>4</sub> solution is injected. A simple solution to the above mentioned drawbacks would be to develop a synthetic protocol that generally keeps the four stage procedure, with all its benefits ('quality' of the product), but which allows for multiple NT syntheses from the same batch of intermediate seeds; in other words we are seeking a protocol in which intermediate seeds are stable over a prolonged time (Figure 1a).

To identify proper conditions for stabilizing the intermediate seeds we first realized that, in the original protocol, if the isotropic overgrowth of the initial seeds is not stopped (by fast addition to the final growth medium), the resulting particles are not suitable for efficient synthesis of NTs.<sup>[11,17]</sup> Thus, we hypothesized that limiting the initial seeds overgrowth by selecting suitable synthetic conditions – not by fast addition – can be advantageous for our purposes. For this reason, we carried out the overgrowth of the initial seeds using 1/3 molar content of Au, as compared to the previous protocol. These synthetic conditions allowed us to achieve spherical Au NPs with 10 ± 2 nm diameter (as determined with the TEM, Figure 1b) with a strong LSPR band centered at 520 nm (Figure 1c). This seed size is consistent with previous report of some of us, in which we show that spherical NPs with diameters 10–20 nm can be used for efficient synthesis of NTs.<sup>[11]</sup> UV-Vis measurements of the seed solution did not reveal any changes in the plasmonic behavior over the course of six days (when kept at 4 °C), indicating high stability. Importantly, TEM imaging enabled us to confirm twin plane formation within the seeds

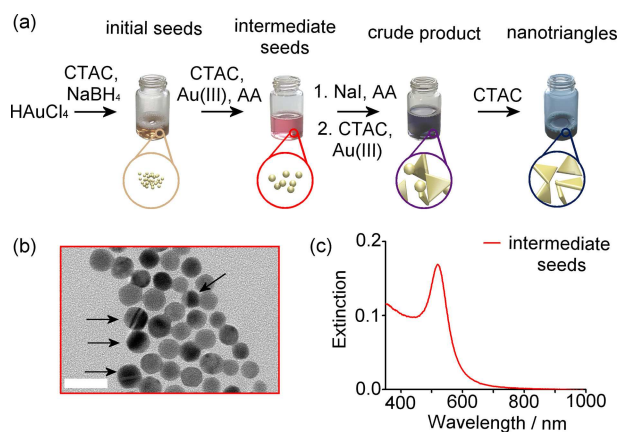


**Figure 1.** Outline of the synthetic protocol and ‘intermediate’ seeds investigation. (a) Graphical representation of a 4-stage synthetic protocol used for the synthesis of gold nanotriangles. Vials with solutions of intermediate products and graphical representation of the intermediate products are shown. (b) TEM micrograph of ‘intermediate’ seeds – nanoparticles with clearly visible twin planes are highlighted. (c) UV-Vis spectroscopy spectrum of an ‘intermediate’ seed suspension. Scale bar: (b) 20 nm.

(indicated by arrows in Figure 1b), which has been shown to be a crucial feature toward symmetry breaking in NTs synthesis.<sup>[17,18]</sup>

## 2.2. Symmetry Breaking, Size Control and Purification of the Product

We then used our intermediate seeds to prepare NTs. For this purpose, we decided to shortly preincubate our intermediate seeds with small amounts of iodide to allow for its adsorption on the surface of the gold seeds, before proceeding with anisotropic overgrowth, since the presence of iodide is known to be crucial for symmetry breaking when growing NTs.<sup>[11,17]</sup> Here, we found that very similar results were obtained for preincubation times from 0 to 90 s as evidenced by UV-Vis spectroscopy investigations of unpurified products (Figure S1). In our hands 45 s of preincubation gave the most reproducible results.

It is worth noting, that in the original protocol iodide addition at the stage of intermediate seeds synthesis increased shape yield of NTs synthesis but was not required for NTs synthesis. However, ‘fast addition’ of the growth solution containing iodide was crucial, since intermediate seeds have to be small enough to allow for symmetry breaking to occur.<sup>[11]</sup>

In trial synthesis we used 100  $\mu\text{L}$  of the intermediate seeds suspension, to which we added iodide and ascorbic acid. After preincubation, the growth solution containing Au(III) and an additional portion of iodide is added under heavy stirring. The reaction mixture is allowed to stir for few seconds and then left undisturbed for formation of the final product. The color of the reaction mixture was observed to slowly develop for few minutes. The whole process is shown in the Supporting Movie 1. UV-Vis spectra collected 2 h after the synthesis (without any purification) is shown in Figure 2a (green curve). TEM micro-

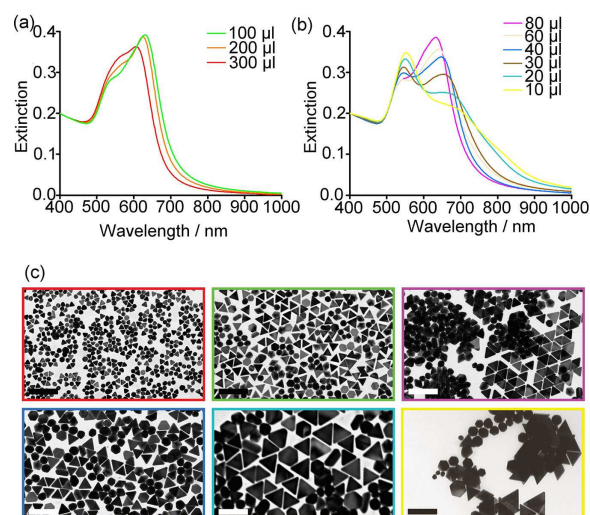


**Figure 2.** Size tunability of NTs – analysis of crude (unpurified) products. (a, b) UV-Vis spectra of reaction mixtures, 2 h after NTs synthesis (without purification); the legends indicate the volume ( $\mu\text{L}$ ) of intermediate seeds used for each sample. (c) TEM micrographs of unpurified products, obtained using different amounts of intermediate seeds. Colors of the frames correspond to colors used in UV-Vis spectra shown in panels a and b. Scale bars: 200 nm.

raphy of this reaction mixture revealed formation of triangular nanoprisms in a mixture with other types of (an)isotropic nanoparticles (Figure 2c). Shape yield of the synthesis was 45 % (Figure S2f). The reaction product was then subject to purification. In analogy to previously developed protocols, we aimed at selective precipitation of NTs by addition of a concentrated CTAC solution, which enables depletion-induced aggregation.<sup>[17]</sup> It has been shown that this method leads not only to purification of the product from other nanoparticle shapes, but also to a narrower size distribution. The amount of CTAC required for NTs purification was estimated on the basis of the depletion interaction energy, as previously proposed.<sup>[17,37,38]</sup> After reaching the desired CTAC concentration, the mixture was left undisturbed for 24 h; after that time, small precipitate was observed at the bottom of the vial and the supernatant changed color from bluish/violet to reddish/pink, suggesting that mainly isotropic NPs remained in suspension. UV-Vis spectra of the purified product is shown in Figure 3a (green curve). TEM micrograph of this reaction mixture revealed formation of triangular nanoprisms,  $60 \pm 4$  nm edge length (Figure 3c).

After we have proved that our stable intermediate seeds can be used to produce gold NTs, we next tackle the issue to control size and tuning optical properties of the produced NTs. We first decided to test the size range of NTs that can be obtained with the new protocol, by simply varying the amount of the seeds added to the final growth solution. To obtain small nanoparticles, 200 and 300  $\mu\text{L}$  of seeds were used in separate reactions. UV-Vis analysis of the reaction mixtures (2 h after the final synthetic step, Figure 2a) revealed that the position of the LSPR maxima blue-shifts with increasing the amount of seeds, suggesting the formation of smaller nanotriangles.<sup>[17]</sup> Indeed,

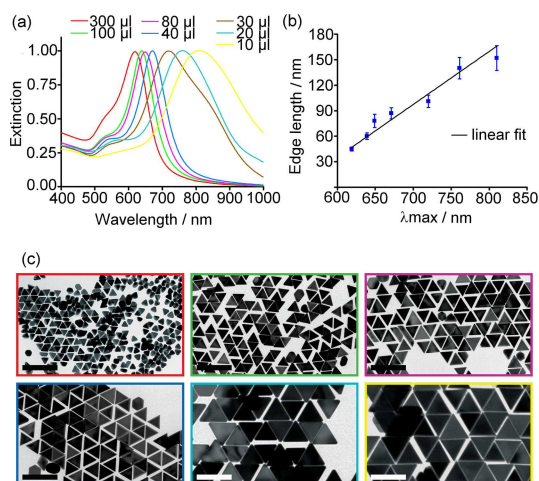


**Figure 3.** Size-tunability of NTs – analysis of purified products. (a) UV-Vis spectra of purified NTs suspensions; labels indicate the volume of intermediate seeds used for each sample; colors of the curves correspond to those in Figure 1. (b) Correlation of LSPR maxima vs. size of purified samples of NTs. (c) TEM micrographs of purified NTs obtained with different amounts of intermediate seeds. Additional TEM micrographs are shown in Figure S4. Scale bars: 200 nm.

TEM analysis of the crude products confirmed the presence of NTs with average edge length 45 nm (Figure 2c, sample 300). Conversely, the use of smaller amounts of intermediate seeds resulted in red-shifted LSPR bands (Figure 2b), but with lower intensity, which may be due to lower shape yield of the reaction as well as depletion-induced precipitation of NTs – since the reaction conditions are the same (CTAC concentration is kept constant), larger NTs are more prone to aggregation. It should be noted that the plasmon band around 540 nm gets more intense, since spherical particles are not affected by the depletion forces. TEM micrographs confirmed the formation of larger NTs with edge length up to 150 nm (Figure 1c).

For most of the produced NTs, a one-step purification with CTAC (concentrations are given in Table S1) was enough to achieve a high-quality product. However, we found that for larger NTs (above 100 nm edge length), a two-step procedure is more effective. In the first step, a higher CTAC concentration produced precipitation of nanotriangles, along with larger by-product particles, leaving smaller ones in the supernatant, which is discarded (Figure S3a). Subsequently, the precipitate is re-dispersed in a solution with lower CTAC concentration, so that only larger NTs or hexagonal plates precipitate and the desired NTs stay in the supernatant (Figure S3b).

UV-Vis spectra and TEM images of the purified products with different sizes, are shown in Figure 3 (additional TEM images are given in Figure S4) and confirm successful purification. With the proposed approach we were able to tune the size of the NTs between  $45 \pm 2.3$  and  $152 \pm 9.5$  nm, which translates to LSPR band maxima ranging from ca. 620 to 810 nm (Table S1). LSPR band maxima shows a linear correlation to the size of NTs, as previously found<sup>[17]</sup> (Figure 3b). LSPR bands of the products obtained using small amounts of seeds (10, 20 and 30 µl, Figure 3a), which correspond to nanotriangles with

size above 100 nm exhibit as shoulder at longer wavelengths which is most probably due to partial contamination with nanoplates (Figure S4h,j) or due to partial, depletion forces driven aggregation of NTs. Interestingly, in all samples the thickness of the produced NTs was relatively constant –  $26 \pm 4$  nm (calculated by measuring thickness of vertically arranged NTs, which are seldom found in the prepared TEM samples, Figure S5). Using this value one can roughly estimate that aspect ratio of these NTs changes from  $\sim 1.7$  (NTs with edge length 45 nm) to  $\sim 5.8$  (NTs with edge length 152 nm). Thus, this method can be viewed as complementary to the previously reported synthesis that relied on the overgrowth of smaller NTs – namely, Kuttner et al. achieved NTs of different sizes but the same aspect ratio.<sup>[19]</sup>

### 2.3. Seed Stability, Reproducibility and Scalability

The main novelty of this work is related to the stability of the intermediate seeds, which is directly connected to the reproducibility and scalability of the proposed protocol. Shown in Figure S6a are UV-Vis spectra of unpurified reaction mixtures (taken 2 h after the synthesis), from syntheses performed over the course of 6 days using the same batch of seeds. Even though there is some variation in the spectral shape, it is mainly related to a slight broadening, indicating that the intermediate seeds are more stable than those previously reported. An even better spectral reproducibility is obtained after purification, as shown in Figure 4a, for purified NTs produced at day 2 and day 6.

With a closer focus on reproducibility, we performed a series of experiments (batches 1–4, Figure 4b), including repetition of the protocol by a different researcher in a different laboratory (experiments were initially performed at CICbiomaGUNE, Spain,

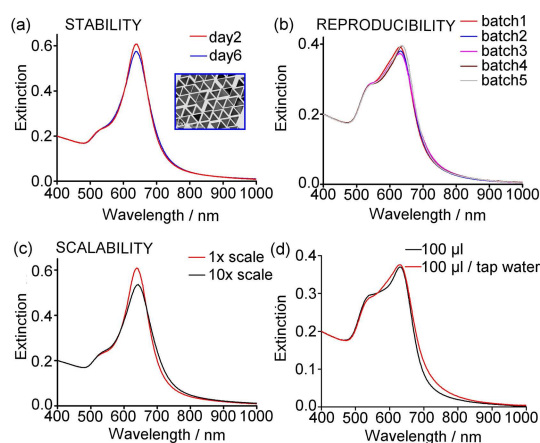


**Figure 4.** User-friendly character of the synthetic protocol. (a) UV-Vis spectra of purified NTs obtained from the same batch of seeds, 24 h (red curve) and 6 days (blue curve) after synthesis of the intermediate seeds. (b) UV-Vis spectra of reaction mixtures obtained in independent experiments; batch 5 (gray curve) was performed in a different laboratory. (c) UV-Vis spectra of purified NTs obtained at 1x the reported scale (red curve) and 10x times larger scale (black curve). (d) UV-Vis spectra of crude reaction mixtures obtained for reactions performed using the outlined protocol (black curve, sample 100) and using tap water at the final growth stage (red curve).

batch 1–4, and then repeated at the University of Warsaw, Poland, batch 5, Figure 4b). UV-Vis spectra of crude reaction mixtures revealed almost no change in all these experiments, confirming a high reproducibility. Finally, we focused on the ability to up-scale the reaction. We carried out a reaction at 10x the regular scale. As shown in Figure 4c, the UV-Vis spectra of the purified product was similar to that achieved for the standard reaction volume.

When up-scaling the reaction, it should be noticed that preparation of larger NTs (above 100 nm edge length) requires the use of slightly (20%) larger amount of intermediate seeds. This problem of scaling up might be due to slower mixing of the larger volumes of solutions, which might affect e.g. kinetics of the reaction or result in differences of the reaction start point in different parts of the reaction mixture.

In the original protocol, ultrapure water was used throughout the synthesis, involving relatively large volumes. Since many laboratories have limited access to ultrapure water supply, they would benefit from developing a procedure that requires only small amounts of ultrapure water. We therefore, in a proof-of-principle manner, explored the possibility to overgrow the intermediate seeds using directly tap water (in our case pH ~7.5, total ion content above 2 mM). Interestingly, both UV-Vis spectra and TEM images confirmed the successful synthesis of well-defined NTs (Figure 4d, Figure S6b). We note that tap water contents will be different from place to place, however, we may safely assume that using distilled water should yield aimed NTs. Still, it is worth to mention, that low/variable quality of water is one of the main sources of irreproducibility in nanoparticle synthesis<sup>[35,36]</sup> and e.g. pH value can affect NTs growth.<sup>[19]</sup>

## 2.4. Self-Assembly into Vertical Arrays

Up-to-date reports on achieving vertical assemblies of NTs rely on drop casting the NT dispersions with different CTAC concentrations.<sup>[9,19]</sup> Along this line, we drop casted purified reaction mixtures of NTs (45 nm side length) from 5 mM CTAC aqueous solutions. To slow down the evaporation of water during the self-assembly process, TEM grids carrying the colloid droplet were placed in a 100% relative humidity environment, achieved by placing the sample within a chamber filled with water. Using this methodology, we were able to achieve few square  $\mu\text{m}$  areas of vertically aligned NTs, as revealed by TEM analysis (Figure 5a). However, such assemblies were mainly found within the coffee ring area, which may result from fast precipitation of colloidal clusters of NTs, forming in solution due to depletion forces. At the same time, in the inner parts of the grid a chaotic distribution of NTs covered by CTAC was mainly observed (Figure 5b). Another issue is related to the washing process required to enable analyte access to the gold surface, i.e. removal of excess CTAC.<sup>[19]</sup> This washing procedure can lead to loosening of the NTs packing or removal of nanoparticles from the substrate, and it would be important to find ways to omit this step. We decided to use a methodology previously developed for gold nanorods<sup>[33]</sup> and hexagonal Ag

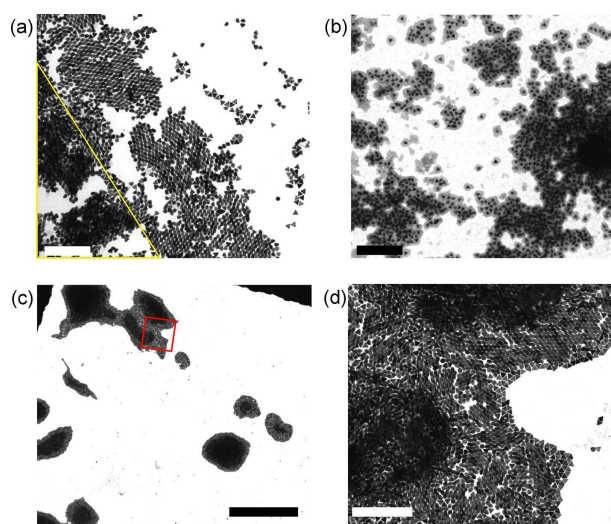


**Figure 5.** Self-assembly of NTs. (a) TEM micrograph of an outer coffee ring region prepared using CTAC; a region with high CTAC accumulation is highlighted in yellow. (b) TEM micrograph from the same TEM grid, in an inner region. (c) TEM micrograph of vertical assemblies made of Au NTs capped with MUDOL. The red square indicates the region shown in higher magnification in panel (d). Additional TEM micrographs of vertical assemblies made of Au NTs capped with MUDOL are shown in Figure S12. Scale bars: (c) 5  $\mu\text{m}$ , (a,b,d) 500 nm.

nanoplates,<sup>[39]</sup> namely, lowering the colloidal stability of NTs suspensions by exchanging the ligands on the NPs surface.

We tested different compounds that have been shown to provide stability of metal NPs in aqueous solutions, namely: PEG-SH (molecular weight 5000 Da), 11-mercaptopundecanoic acid, captopril<sup>[39]</sup> and 11-mercaptopundecyl hexa(ethylene glycol) (MUDOL, Figure S7). Ligand exchange reactions were performed to introduce these molecules onto the NTs surface, while the CTAC concentration was lowered to below 50  $\mu\text{M}$ . The particles were then drop casted in the same manner as those stabilized with CTAC. TEM analysis of the assemblies formed with the three former ligands are shown in Figures S8–S10. In all these cases, a portion of the NTs did assemble into vertical arrays, though co-existing with horizontally oriented areas. On the contrary, in the case of MUDOL, vertical assemblies were obtained over hundreds of square microns large areas with about 80% of the nanoparticles oriented orthogonal to the substrate (Figure 5b, c). Within such vertical assemblies, NTs form one to few layer thick i-honeycomb lattices,<sup>[9]</sup> with  $a = 33 \pm 1.7$  nm and  $b = 60 \pm 2.0$  nm (Figure S11). Importantly, mainly 1- or 2-layer thick assemblies were obtained, which are known to be of major interest from an application point of view.<sup>[33]</sup> In contrast to the sample shown in Figure 4a, these assemblies were not covered by a thick layer of CTAC, further favoring their potential for practical applications.

## 3. Conclusions

We have developed an improved method for the synthesis of gold nanotriangles. Overall, the procedure was simplified to

facilitate its use by a wide community of researchers, not necessarily requiring prior experience in anisotropic NPs synthesis. The developed method is scalable, reproducible and allows for a broader range of NTs size, as compared to the current state-of-the-art seed-mediated methods. Additionally, only small amounts of pure water are required for the synthesis (for the seeds), showing robustness in the growth steps. Finally, the quality of the product allowed us to demonstrate efficient assembly into interlocked, vertical aggregates of NTs, over large areas, and therefore with potential for practical applications.

## Experimental Section

### Materials

Tetrachloroauric acid ( $\text{HAuCl}_4 \geq 99\%$ ), hexadecyltrimethylammonium chloride (CTAC, 25 wt% in water), sodium borohydride ( $\text{NaBH}_4$ ), L-ascorbic acid (AA,  $\geq 99\%$ ), 11-mercaptoundecanoic acid (95%, Captopril  $\geq 98\%$ , poly(ethylene glycol) (PEG-SH) 5000 Da and 11-mercaptoundecyl hexa(ethylene glycol) (MUDOL) 90% were purchased from Sigma-Aldrich and used without any purification.

### Synthesis of the Initial Seeds

25  $\mu\text{L}$  of  $\text{HAuCl}_4$  50 mM solution was added to 4.7 mL of a CTAC 100 mM solution and stirred for 2–3 min. Then, 300  $\mu\text{L}$  of a freshly prepared 10 mM  $\text{NaBH}_4$  solution was injected under vigorous stirring and further stirred less vigorously for 2 h. The reaction mixture should have a pale brown color. Typical problems that occur at this stage concern the addition of an insufficient amount of  $\text{NaBH}_4$  due to its hygroscopic nature and quick decomposition. Thus, if the final reaction is unsuccessful we recommend using 24.5  $\mu\text{L}$  of  $\text{HAuCl}_4$  50 mM solution instead of 25  $\mu\text{L}$ . When learning the protocol we recommend setting up 2–3 reactions to achieve the initial seeds visually inspect them and continue the protocol with each batch. By assessing quality of NTs achieved with them it is possible to learn to prepare the optimal batch of the initial seeds. To confirm that gold (III) ions were reduced completely, UV-VIS measurement of seeds solution can be implemented to check the concentration of Au(0). If the absorbance at 400 nm wavelength is below 0.6 (indicating Au(0) concentration below 0.25 mM), it means that the amount of added borohydride was lower than expected (assuming the  $\text{HAuCl}_4$  amount was correct).<sup>[35]</sup>

### Synthesis of the Intermediate Seeds

16.6  $\mu\text{L}$  of 50 mM  $\text{HAuCl}_4$  solution and 20  $\mu\text{L}$  of 100 mM AA solution are added to 10 mL of a 25 mM CTAC solution. Then, under vigorous stirring, 100  $\mu\text{L}$  of the initial seeds solution is added to the mixture. After 3 seconds of stirring the vial is put aside and left undisturbed for 24 h.

### Final Product Synthesis

Vial 1: AA (104  $\mu\text{L}$ , 100 mM) and NaI (40  $\mu\text{L}$ , 10 mM) solutions are added to 10.2 mL of CTAC (50 mM) and then 100  $\mu\text{L}$  of intermediate seed solution is added rapidly. The reaction is stirred for 45 s before addition of vial 2. Vial 2:  $\text{HAuCl}_4$  (130  $\mu\text{L}$ , 50 mM), deionized water (390  $\mu\text{L}$ ) and NaI (40  $\mu\text{L}$ , 10 mM) are mixed together by hand shaking. Procedure: Solution from vial 2 is added to the mixture in vial 1 under vigorous stirring 45 s after intermediate seed solution addition.

### Purification

A CTAC solution of appropriate concentration (see below) was added to the crude reaction mixture. Amounts of the CTAC were calculated based on the original procedure for NTs synthesis. For example, NTs with edge length of 60 nm were purified by increasing the CTAC concentration directly in the reaction mixture (at least 12 h after the synthesis) to about 200 mM, while for smaller NTs (45 nm edge length) a CTAC concentration above 350 mM was used. For triangles with edge length above 120 nm it is better to discard the supernatant from the reaction mixture (in which CTAC concentration is 50 mM) and then re-disperse the precipitate in a less concentrated CTAC solution. For large NTs it might also be beneficial to implement a second step purification in which the precipitate from the first step is dispersed in a CTAC solution of very low concentration, left overnight and the precipitate containing larger impurities is then discarded. For example, NTs with edge length of 140 nm were purified by re-dispersing the precipitate from the reaction mixture in 35 mM CTAC (first purification step, precipitate was collected) and then in 5 mM CTAC (second step, supernatant was collected). See Figure S2 for details.

### Self-Assembly

For NTs stabilized with CTAC, nanoparticles were drop casted from a NTs dispersion in 5 mM CTAC. For NTs@MUDOL the self-assembly procedure started with a ligand exchange reaction. A solution of NTs (0.5 mM Au, 2 mL) was mixed with excess ligand (100  $\mu\text{L}$ , 1 mM), and left under gentle stirring for 24 h. The material was then centrifuged and washed twice with water (2 mL each time) and suspended in a small amount of pure water. In all cases 3  $\mu\text{L}$  of the material were drop casted onto a TEM grid and left in a 100% relative humidity environment (TEM grid placed on a substrate floating on water in a closed vessel), for slow droplet evaporation.

### Acknowledgements

The work was supported by the MOBILITY Plus programme (agreement No. 1259/MOB/IV/2015/0) financed by the Polish Ministry of Science and Higher Education.

### Conflict of Interest

The authors declare no conflict of interest.

**Keywords:** triangular nanoplates · anisotropic nanoparticles · symmetry breaking · vertical assemblies · tunable plasmon

- [1] C. Hamon, M. Henriksen-Lacey, A. La Porta, M. Rosique, J. Langer, L. Scarabelli, A. B. S. Montes, G. González-Rubio, M. M. de Pancorbo, L. M. Liz-Marzán, L. Basabe-Desmonts, *Adv. Funct. Mater.* **2016**, *26*, 8053–8061.
- [2] L. Lin, X. Peng, M. Wang, L. Scarabelli, Z. Mao, L. M. Liz-Marzán, M. F. Becker, Y. Zheng, *ACS Nano* **2016**, *10*, 9659–9668.
- [3] M. Wang, A. Krasnok, T. Zhang, L. Scarabelli, H. Liu, Z. Wu, L. M. Liz-Marzán, M. Terrones, A. Alù, Y. Zheng, *Adv. Mater.* **2018**, *30*, 1705779.
- [4] M. Wang, W. Li, L. Scarabelli, B. B. Rajeeva, M. Terrones, L. M. Liz-Marzán, D. Akinwande, Y. Zheng, *Nanoscale* **2017**, *9*, 13947–13955.

- [5] L. Lin, M. Wang, X. Peng, E. N. Lissek, Z. Mao, L. Scarabelli, E. Adkins, S. Coskun, H. E. Unalan, B. A. Korgel, L. M. Liz-Marzán, E.-L. Florin, Y. Zheng, *Nat. Photonics* **2018**, *12*, 195–201.
- [6] S. R. Bhattarai, P. J. Derry, K. Aziz, P. K. Singh, A. M. Khoo, A. S. Chadha, A. Liopo, E. R. Zubarev, S. Krishnan, *Nanoscale* **2017**, *9*, 5085–5093.
- [7] J. Reguera, J. Langer, D. Jiménez de Aberasturi, L. M. Liz-Marzán, *Chem. Soc. Rev.* **2017**, *46*, 3866–3885.
- [8] B. B. Rajeeva, D. S. Hernandez, M. Wang, E. Perillo, L. Lin, L. Scarabelli, B. Pingali, L. M. Liz-Marzán, A. K. Dunn, J. B. Shear, Y. Zheng, *Adv. Sci.* **2015**, *2*, 28–30.
- [9] J. Kim, X. Song, F. Ji, B. Luo, N. F. Ice, Q. Liu, Q. Zhang, Q. Chen, *Nano Lett.* **2017**, *17*, 3270–3275.
- [10] P. Mitchell, P. Lane, F. Racimo, J. Helm, *Science* **2017**, *356*, 1120–1121.
- [11] G. González-Rubio, T. M. De Oliveira, T. Altantzis, A. La Porta, A. Guerrero-Martínez, S. Bals, L. Scarabelli, L. M. Liz-Marzán, *Chem. Commun.* **2017**, *53*, 11360–11363.
- [12] F. Zhang, J. Zhu, H.-Q. An, J.-J. Li, J.-W. Zhao, *J. Mater. Chem. C* **2016**, *4*, 568–580.
- [13] C. Kuttner, M. Mayer, M. Dulle, A. I. Moscoso, J. M. López-Romero, S. Förster, A. Fery, J. Pérez-Juste, R. Contreras-Caceres, *ACS Appl. Mater. Interfaces* **2018**, *10*, 11152–11163.
- [14] Y. Huang, A. R. Ferhan, Y. Gao, A. Dandapat, D.-H. Kim, *Nanoscale* **2014**, *6*, 6496–6500.
- [15] G. Wang, S. Tao, Y. Liu, L. Guo, G. Qin, K. Ijiri, M. Maeda, Y. Yin, *Chem. Commun.* **2016**, *52*, 398–401.
- [16] B. Tangeysh, K. M. Tibbetts, J. H. Odhner, B. B. Wayland, R. J. Levis, *Langmuir* **2017**, *33*, 1, 243–252.
- [17] L. Scarabelli, M. Coronado-Puchau, J. J. Giner-Casares, J. Langer, L. M. Liz-Marzán, *ACS Nano* **2014**, *8*, 5833–5842.
- [18] J. E. Millstone, S. J. Hurst, G. S. Métraux, J. I. Cutler, C. A. Mirkin, *Small* **2009**, *5*, 646–664.
- [19] C. Kuttner, M. Mayer, M. Dulle, A. Moscoso, J. M. López-Romero, S. Förster, A. Fery, J. Pérez-Juste, R. Contreras-Cáceres, *ACS Appl. Mater. Interfaces* **2018**, *10*, 11152–11163.
- [20] P. Yang, J. Zheng, Y. Xu, Q. Zhang, L. Jiang, *Adv. Mater.* **2016**, *28*, 10508–10517.
- [21] S. Yu, J. a. Hachtel, M. F. Chisholm, S. T. Pantelides, A. Laromaine, A. Roig, *Nanoscale* **2015**, *7*, 14039–14046.
- [22] Y. Zhai, J. S. DuChene, Y.-C. Wang, J. Qiu, A. C. Johnston-Peck, B. You, W. Guo, B. DiCiccio, K. Qian, E. W. Zhao, *Nat. Mater.* **2016**, *15*, 889–895.
- [23] F. Shaik, W. Zhang, W. Niu, *J. Phys. Chem. C* **2017**, *121*, 9572–9578.
- [24] L. Chen, F. Ji, Y. Xu, L. He, Y. Mi, F. Bao, B. Sun, X. Zhang, Q. Zhang, *Nano Lett.* **2014**, *14*, 7201–7206.
- [25] M. Grzelczak, J. Pérez-Juste, P. Mulvaney, L. M. Liz-Marzán, *Chem. Soc. Rev.* **2008**, *37*, 1783–1791.
- [26] N. Li, P. Zhao, D. Astruc, *Angew. Chem. Int. Ed.* **2014**, *53*, 1756–1789; *Angew. Chem.* **2014**, *126*, 1784–1818.
- [27] C. R. Laramy, L.-K. Fong, M. R. Jones, M. N. O'Brien, G. C. Schatz, C. A. Mirkin, *Chem. Phys. Lett.* **2017**, *683*, 389–392.
- [28] M. A. Huergo, L. J. Giovanetti, A. A. Rubert, C. A. Grillo, M. S. Moreno, F. G. Requejo, R. C. Salvarezza, C. Vericat, *Appl. Surf. Sci.* **2019**, *464*, 131–139.
- [29] E. Cortés, W. Xie, J. Cambiasso, A. S. Jermyn, R. Sundararaman, P. Narang, S. Schlücker, S. A. Maier, *Nat. Commun.* **2017**, *8*, 14880.
- [30] P. Li, Y. Li, Z.-K. Zhou, S. Tang, X.-F. Yu, S. Xiao, Z. Wu, Q. Xiao, Y. Zhao, H. Wang, P. K. Chu, *Adv. Mater.* **2016**, *28*, 2511–2517.
- [31] C. Hamon, L. M. Liz-Marzán, *Chem. Eur. J.* **2015**, *21*, 9956–9963.
- [32] C. Hamon, S. Novikov, L. Scarabelli, L. Basabe-Desmonts, L. M. Liz-Marzán, *ACS Nano* **2014**, *8*, 10694–10703.
- [33] C. Hamon, S. M. Novikov, L. Scarabelli, D. M. Solís, T. Altantzis, S. Bals, J. M. Taboada, F. Obelleiro, L. M. Liz-Marzán, *ACS Photonics* **2015**, *2*, 1482–1488.
- [34] C. Hamon, M. Postic, E. Mazari, T. Bizien, C. Dupuis, P. Even-Hernandez, A. Jimenez, L. Courbin, C. Gosse, F. Artzner, V. Marchi-Artzner, *ACS Nano* **2012**, *6*, 4137–4146.
- [35] L. Scarabelli, A. Sánchez-Iglesias, J. Pérez-Juste, L. M. Liz-Marzán, *J. Phys. Chem. Lett.* **2015**, *6*, 4270–4279.
- [36] G. González-Rubio, V. Kumar, P. Llombart, P. Díaz-Núñez, E. Bladt, T. Altantzis, S. Bals, O. Peña-Rodríguez, E. G. Noya, L. G. MacDowell, A. Guerrero-Martínez, L. M. Liz-Marzán, *ACS Nano* **2019**, acsnano.8b09658.
- [37] K. Park, H. Koerner, R. A. Vaia, *Nano Lett.* **2010**, *10*, 1433–1439.
- [38] K. L. Young, M. L. Personick, M. Engel, P. F. Damasceno, S. N. Barnaby, R. Bleher, T. Li, S. C. Glotzer, B. Lee, C. A. Mirkin, *Angew. Chem. Int. Ed.* **2013**, *52*, 13980–13984; *Angew. Chem.* **2013**, *125*, 14230–14234.
- [39] N. Cathcart, V. Kitaev, *ACS Nano* **2011**, *5*, 7411–7425.

Manuscript received: March 5, 2019

Revised manuscript received: April 11, 2019